

Novel and Facile Synthesis of Nano SnO₂ with Various Morphologies by Electric Current Stressing

Li Wangyun, Cao Shanshan, Zhang Xinping

South China University of Technology, Guangzhou 510640, China

Abstract: Nano tin oxide (SnO₂) was synthesized by a novel, fast and facile approach through applying electric current of high density to a line-type joint specimen consisting of a high tin-content alloy between two pieces of conductor (copper or nickel). The fabricated SnO₂ shows various morphologies, such as branch-like, pine-leaf-like, grass-like and batting-like, and has the tetragonal rutile structure confirmed by scanning electron microscopy, energy dispersive X-ray spectroscopy and Raman spectrum. The present work has not only offered a facile and novel method for fabricating SnO₂ of various morphologies, but also provided an inspiring yet practical idea as well as technical possibilities for preparation of other functional oxide materials.

Key words: SnO₂; electric current stressing; oxidation; microstructure; Raman

Tin oxide (SnO₂) is a very important n-type semiconductor with a wide band-gap of 3.6 eV (at 300 K). The excellent electrical, optical, and electrochemical properties of SnO₂ allow it to be widely applied in various technological areas, such as solid state gas sensor material, oxidation catalyst, transparent conductor, and lithium ion batteries^[1-3]. It is found that the properties of SnO₂, especially the nano-sized one, depend strongly on its morphology^[4,5]. Several conventional methods were used to prepare SnO₂ with various morphologies, such as grass-like^[5], fishbone-like^[6], pine-leaf-like^[7], flower-like^[8-11] and dandelion-like^[12] or chestnut-like^[13], honeycomb^[14], horseshoe-shaped with annulus-like^[15], which include thermal deposition, physical vapor deposition, chemical vapor deposition, vapor-liquid-solid growth, vapor-solid growth, oxide assisted growth, spray pyrolysis, wet chemical synthesis, electrospinning^[2], hydrothermal synthesis^[9-11] and detonation synthesis^[16], as well as the recently developed methods based on electron stimulated oxidation^[17] and direct current arc discharge^[18]. However, none of the above methods can be used to synthesize SnO₂ with diverse morphologies and scales by a simple one-step process^[4], and there is no work reporting synthesis of SnO₂ by using electric current stressing.

In this paper, we report the synthesis of SnO₂ with various

morphologies and scales by a novel, fast and facile approach through applying direct electric current of high density to a specimen consisting of a high tin-content alloy between two pieces of conductive metals (copper or nickel).

1 Experiment

A high tin-content alloy, Sn-3.0Ag-0.5Cu (96.5%Sn, 3.0%Ag, 0.5%Cu, mass fraction), was used as an interlayer to realize the joining of oxygen-free copper to copper wires (or copper to nickel wires) with a diameter of 300 μm by a reflow process on a BGA rework machine (RD-300)^[19,20]. Then, the above reflowed line-type sandwich structure Cu/Sn-3.0Ag-0.5Cu/Cu (or Cu/Sn-3.0Ag-0.5Cu/Ni) joint specimen was fixed by clamps in a furnace with temperature holding accuracy of ≤0.1 °C, and the clamps were well insulated using insulating plates. The direct electric current with a density of 1.0×10⁴ A/cm² was supplied by a constant-current power supply (SHEKONIC). The schematic of the experiment set-up used in this study is shown in Fig.1. During the experiment, once the furnace temperature reached a pre-programmed value, such as 216 °C, the electric current was immediately applied to the specimen. After the specimen was electro-thermally loaded to fracture, it was taken away carefully from the clamps, and the as-obtained product on surface of the

Received date: September 7, 2017

Foundation item: National Natural Science Foundation of China (51275178); Science and Technology Planning Project of Guangdong Province (2014A010105023)
Corresponding author: Zhang Xinping, Ph. D., Professor, School of Materials Science and Engineering, South China University of Technology, Guangzhou 510640, P. R. China, Tel: 0086-20-22236396, E-mail: mexzhang@scut.edu.cn

Copyright © 2018, Northwest Institute for Nonferrous Metal Research. Published by Elsevier BV. All rights reserved.

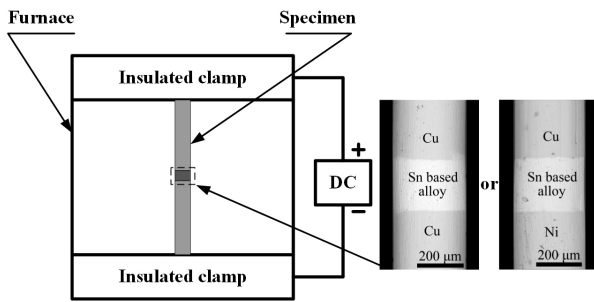


Fig.1 Experiment set-up with electro-thermal coupled loads

fractured specimen was characterized by scanning electron microscope (ProX, Phenom), energy dispersive X-ray spectroscopy (EDS) and Raman spectrometer.

2 Results and Discussion

Fig.2 shows SEM images of the fractured specimen (Fig. 2a and 2b) and the as-obtained product with various morphologies on the fracture surface (Fig.2c~2f). Clearly, the size of the product varies over a wide range from micro- to nano- scale, and its morphology changes greatly. For example, the product shows branch-like with the main branches in micro-scale, as shown in Fig.2c, and presents pine-leaf-like with main rods in a length of about tens of micrometers and pine-leaves in nano-scale, as shown in Fig. 2d. Notably, the product turns into nano-scale completely when exhibiting grass-like or batting-like morphologies, see Fig.2e and 2f.

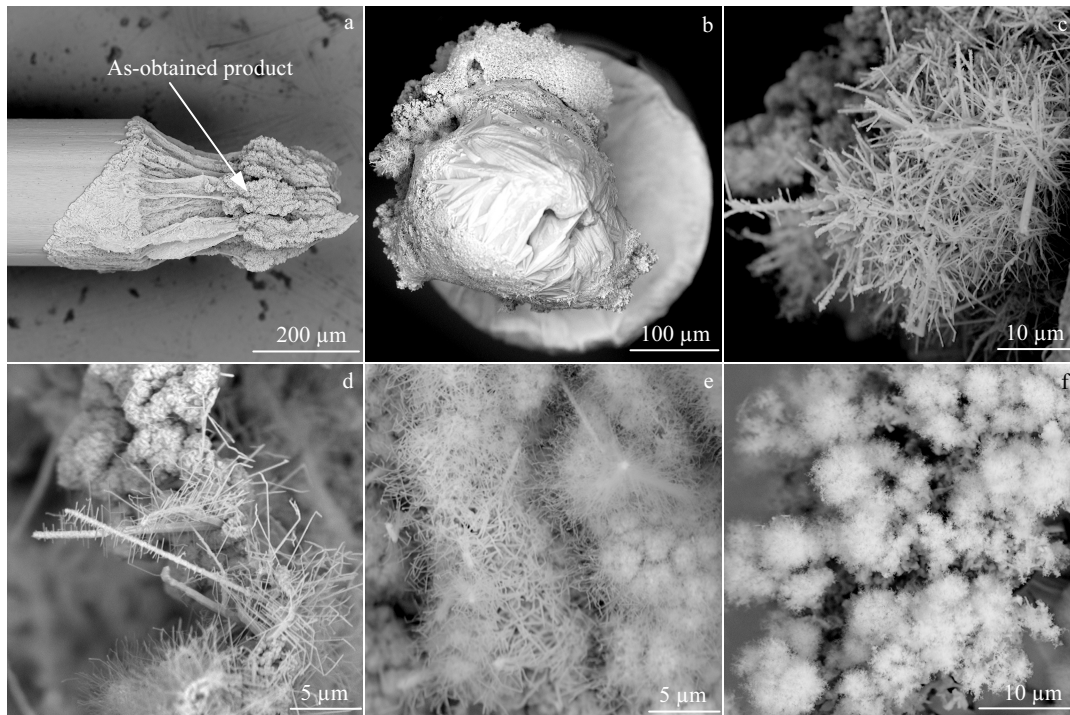


Fig.2 SEM images of side view (a) and top view (b) of the fractured specimen and the as-obtained product with various morphologies of branch-like (c), pine-leaf-like (d), grass-like (e) and batting-like (f) on the fracture surface

Fig.3 shows EDS and Raman spectrum of the as-obtained product, which is composed of Sn and O with a Sn:O ratio close to 1:2, as presented in Fig.3a. Raman spectra show three fundamental Raman scattering peaks at 471.4, 630.2 and 772.2 cm^{-1} , see Fig.3b, which should be attributed to the E_g , A_{1g} and B_{2g} modes of SnO_2 crystal, respectively, based on excellent consistency with those of a rutile SnO_2 crystal^[21-23]. Since Raman signals of SnO_2 are quite different from those of SnO ^[24-26], thus Raman spectroscopy has been widely applied in previous studies to differentiate these two phases^[21-27]. Therefore, the as-obtained product is confirmed as SnO_2 from both the composition and crystal structure.

The as-obtained SnO_2 is owing to the oxidation of Sn in Sn-3.0Ag-0.5Cu solder alloy, which contains 96.5% Sn. On current stressing of the specimen with a high current density of $1.0 \times 10^4 \text{ A/cm}^2$ at 216 °C, Joule heating induced temperature is higher than the nominal melting temperature of Sn-3.0Ag-0.5Cu solder (217.1 °C). However, since the volume of the solder matrix in the specimen is so small that the temperature in the solder matrix can hardly be accurately measured or detected by experimental approaches. Therefore, in order to ascertain the Joule heating induced temperature in the joint specimen during current stressing process, finite element (FE) simulation analysis was performed using ANSYS 15.0. The simulation results show that the temperature can be as high as 255 °C in the solder matrix of Cu/Sn-3.0Ag-0.5Cu/Cu joint specimen, as presented in Fig.4a, while being above 273 °C in the Cu/Sn-3.0Ag-0.5Cu/Ni joint specimen, as shown in Fig.4b.

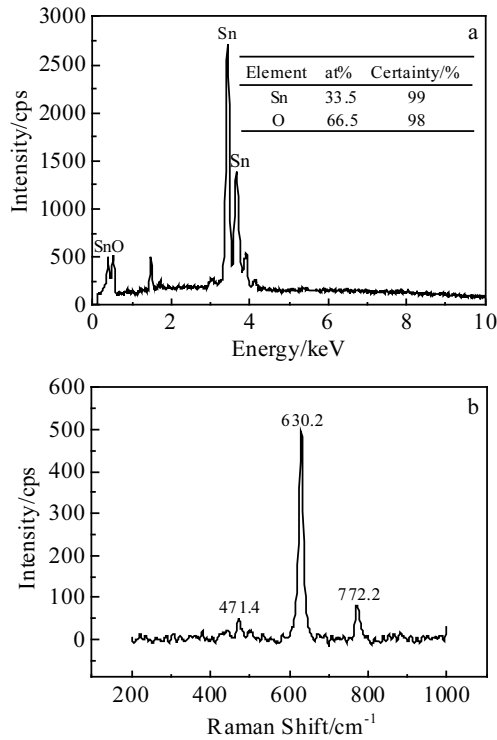


Fig.3 EDS spectrum (a) and Raman spectrum (b) of the as-obtained product on surface of the fractured specimen

It is worth indicating that the higher temperature in the latter specimen is attributed to the higher electrical resistance but lower heat conductivity of Ni and Ni₃Sn₄ as compared to Cu and Cu₆Sn₅, respectively^[28].

Actually, once the electric current is applied to the specimen, the solder matrix melts immediately, resulting in fast fracture in the solder matrix with a cup-cone shape fracture mode, as shown in Fig.2a. It is just at the fracture moment that SnO₂ is formed by the following process and mechanism, as also illustrated in Fig.5. Firstly, after applying electric current to the as-prepared joint specimen as shown in Fig.5a, current

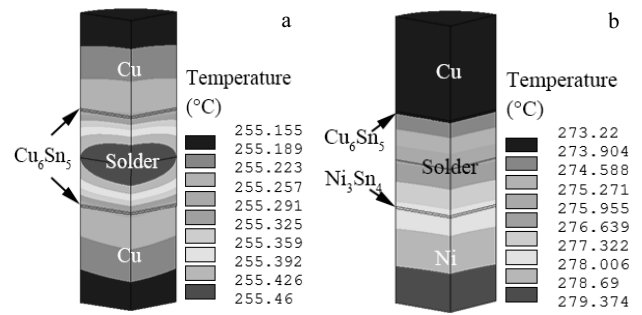


Fig.4 Simulation results of temperature distribution in Cu/Sn-3.0Ag-0.5Cu/Cu joint specimen (a) and Cu/Sn-3.0Ag-0.5Cu/Ni joint specimen (b) under electric current stressing with a density of 1.0×10^4 A/cm² at 216 °C (where one-fourth, i.e., 1/4th, symmetric model is used when considering the axial symmetry of the solder joint)

stress and Joule heating result in the necking of the solder matrix, which in turn induces an extremely severe current crowding at the necking part of the solder matrix, as illustrated in Fig. 5b. Subsequently, the necking part melts and the joint specimen separates, as shown in Fig. 5c, and simultaneously a transient flash arises in the very small gap formed at the moment of occurrence of fracture and the flashing spark can be observed clearly during the test. Essentially, the flash spark is like arc discharge, which induces high temperature^[18,29,30] and makes Sn atoms be oxidized instantaneously^[18], the ionized oxygen around the spark^[31] can enhance the oxidation of Sn, and thus the following reaction can occur: $\text{Sn} + \text{O}_2 \rightarrow \text{SnO}_2$; the various morphologies of SnO₂ can be a result of fast flowing and spraying of the molten Sn and the oriented growth of SnO₂, as illustrated in Fig.5d and 5e, which can be verified by the morphology of SnO₂ shown in Fig.2c and 2d, and further evidenced by formation of some isolated SnO₂ nano-wires among the orientedly grown ones, as shown in Fig.6a, and notably even some SnO₂ nano-wires are attached on

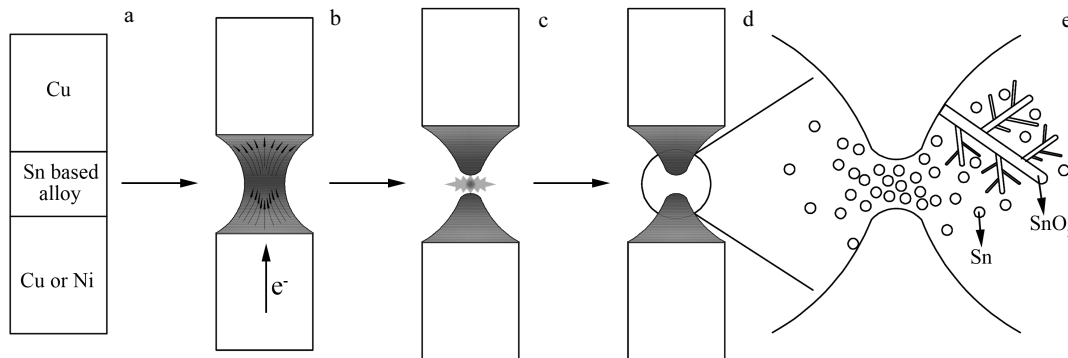


Fig.5 Schematic of the main formation process and mechanism of SnO₂ under electric current stressing: (a) an as-prepared joint specimen before applying electric current, (b) necking of the solder matrix due to current stressing and Joule heating, (c) melting and separating of the necking part as well as emerging of a transient flash and forming of the flashing sparks, (d, e) formation of various morphologies of SnO₂ due to fast flowing and spraying of the molten Sn as well as the oriented growth of SnO₂

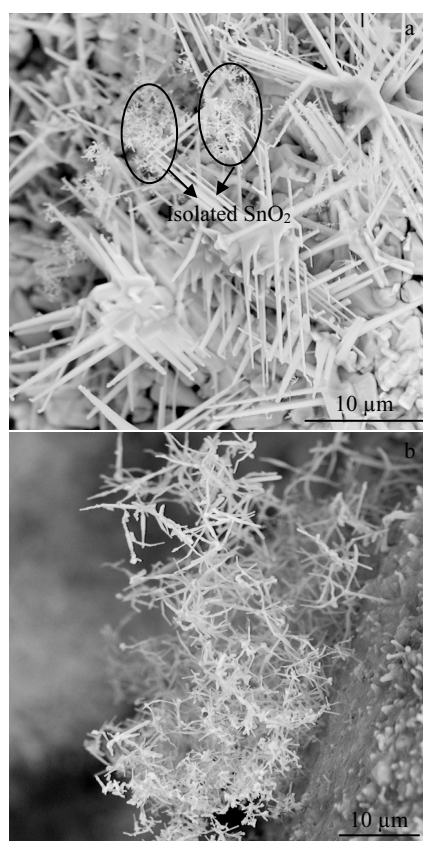


Fig.6 SEM images of SnO₂: (a) orientedly grown SnO₂ affiliated with some isolated SnO₂ and (b) isolated SnO₂ on the surface of the solder matrix

the surface of the solder matrix, see Fig.6b. The above results indicate that the vapor-solid (VS) mechanism also contributes to the formation of SnO₂. During the flash spark process, some Sn atoms in the solder matrix are evaporated and oxidized to form SnO₂ instantaneously due to high temperature. The formed SnO₂ nuclei at high temperature will probably attach to another at a point and accumulate to be a cluster. Subsequently, SnO₂ cluster will accept more nuclei at preferential orientation, resulting in the formation of isolated SnO₂ nano-wires. But Sn in the bulk solder alloy can not evaporate as easily as that of Sn powder under arc discharge^[18]. Thus, the vapor-solid mechanism should not be the dominant growth mechanism of SnO₂ in the present study. Nevertheless, the newly formed SnO₂ on surface of the molten Sn (or solder alloy) can act as catalyst to accelerate the oxidization of inner Sn in the bulk solder alloy^[11,17]. Moreover, the flash spark induced turbulence in the molten solder brings fresh solder surfaces exposing to the high-temperature air, which promotes the oxidization of Sn and formation of SnO₂ with various morphologies and scales.

3 Conclusions

1) SnO₂ with various morphologies and scales has been

successfully synthesized by electro-thermally loading a joint specimen consisting of a high tin-content solder alloy between two pieces of copper or nickel.

2) The synthesis of SnO₂ is realized by the oxidation of Sn in the tin-content alloy using the high temperature and ionized oxygen induced by flashing spark occurring at the fracture moment of the joint specimen.

3) The various morphologies of SnO₂ mainly result from fast flowing and spraying of the molten Sn and the oriented growth of SnO₂.

4) The method developed and presented in this work has also provided an inspiring idea and technical reference, as well as a possible new scheme for preparation of other functional oxide materials.

References

- 1 Batzill M, Diebold U. *Progress in Surface Science*[J], 2005, 79: 47
- 2 Das S, Jayaraman V. *Progress in Materials Science*[J], 2014, 66: 112
- 3 Deng Y F, Fang C C, Chen G H. *Journal of Power Sources*[J], 2016, 304: 81
- 4 Lei D N, Zhang M, Hao Q Y et al. *Materials Letters*[J], 2011, 65: 1154
- 5 Wei J, Xue S L, Xie P et al. *Materials Letters*[J], 2015, 158: 322
- 6 Hu J Q, Bando Y, Golberg D. *Chemical Physics Letters*[J], 2003, 372: 758
- 7 Dee C F, Tiong T Y, Varghese B et al. *Journal of Experimental Nanoscience*[J], 2014, 9: 913
- 8 Zhang H, Zeng W, Hao J H et al. *Materials Letters*[J], 2015, 145: 133
- 9 Zhang M, Zhen Y H, Sun F H et al. *Materials Science and Engineering B*[J], 2016, 209: 37
- 10 Liu Y L, Huang J, Yang J D et al. *Solid-State Electronics*[J], 2017, 130: 20
- 11 Gao F, Li Y H, Zhao Y P et al. *Journal of Alloys and Compounds*[J], 2017, 703: 354
- 12 Wei J, Xue S L, Xie P et al. *Materials Letters*[J], 2015, 159: 489
- 13 Yang L, Dai T, Wang Y C et al. *Nano Energy*[J], 2016, 30: 885
- 14 Wang L L, Li Z J, Zhao C Z et al. *Journal of Alloys and Compounds*[J], 2016, 682: 170
- 15 Wang Y L, Liu C, Wang L et al. *Sensors and Actuators B: Chemical*[J], 2017, 240: 1321
- 16 Yan H H, Wu L S, Li X J et al. *Rare Metal Materials and Engineering*[J], 2013, 42(7): 1325 (in Chinese)
- 17 Li C F, Liu Z Q. *Nanotechnology*[J], 2013, 24: 205 303
- 18 Su Y J, Zhang J, Zhang L L et al. *Journal of Nanoscience and Nanotechnology*[J], 2013, 13: 1078
- 19 Li W Y, Jin H., Yue W et al. *J Mater Sci: Mater Electron*[J], 2016, 27: 13 022
- 20 Zhang Xiping, Li Wangyun, Zhou Mingbo. *China Patent*, CN201610930996.5[P]. 2016 (in Chinese)
- 21 Zhang M, Zhen Y H, Sun F H et al. *Materials Science and En-*

- gineering B[J], 2016, 209: 37
- 22 Lavanya N, Sekar C, Fazio E et al. *International Journal of Hydrogen Energy*[J], 2017, 42: 10 645
- 23 Aragon F H, Aquino J C R, Gomes N C S et al. *Journal of the European Ceramic Society*[J], 2017, 37: 3375
- 24 Bagherian S, Zak A K. *Materials Science in Semiconductor Processing*[J], 2016, 56: 52
- 25 Palacios-Padros A, Cabllero-Briones F, Diez-Perez I et al. *Electrochimica Acta*[J], 2013, 111: 837
- 26 Sharma A, Varshney M, Verma K D et al. *Nuclear Instruments and Methods in Physics Research B*[J], 2013, 308: 15
- 27 Wei J, Xue S L, Xie P et al. *Applied Surface Science*[J], 2016, 376: 172
- 28 Siewert T, Liu S, Smith D R et al. *Database for Solder Properties with Emphasis on New Lead-free Solders, Properties of Lead-free Solders, Release 4.0*[M]. Colorado: National Institute of Standards and Technology & Colorado School of Mines, 2002, 23
- 29 Su Y J, Wei H, Yang Z et al. *Journal of Nanoparticle Research*[J], 2011, 13: 3229
- 30 Su Y J, Wei H, Zhou Z H et al. *Materials Letters*[J], 2011, 65: 100
- 31 Lancaster J F. *Physics in Technology*[J], 1984, 15: 73

电流加载法制备多形貌纳米 SnO₂

李望云, 曹姗姗, 张新平

(华南理工大学, 广东 广州 510640)

摘要: 通过对两端为 Cu (或 Ni) 导体、中间层为高 Sn 合金的三明治结构线型钎焊接头试件加载高密度电流, 创新性地实现了纳米 SnO₂ 的快速、便捷制备。经 SEM、EDX 和拉曼光谱分析表征确认所得 SnO₂ 为四方金红石结构, 具有多种形貌, 如枝状、针叶状、草丛状和棉絮状。本研究所发展的制备方法不仅可快速、高效地制备多形貌多尺度 SnO₂, 还可为其它功能金属氧化物材料的制备提供有效的思路参考和技术方法借鉴。

关键词: SnO₂; 电流加载; 氧化; 微观组织; 拉曼光谱

作者简介: 李望云, 男, 1989 年生, 博士, 华南理工大学材料科学与工程学院, 广东 广州 510640, 电话: 020-22236396, 传真: 020-22236393, E-mail: l.wangyun@mail.scut.edu.cn